Fuzzy rulebase parameter determination for stabilized KH interpolation based detection of colorectal polyps on colonoscopy images

Brigita Sziová
Department of Information Technology
Széchenyi István University
Győr, Hungary
Email: szi.brigitta@sze.hu
https://orcid.org/0000-0001-6400-2767

Raneem Ismail
Széchenyi István University
Győr, Hungary
Email: raneemismail90@gmail.com

Ferenc Lilik
Department of Telecommunications
Széchenyi István University
Győr, Hungary
Email: lilikf@sze.hu
https://orcid.org/0000-0001-8744-1199

László T. Kóczy
Department of Information Technology
Széchenyi István University
Budapest University of Technology and Economics
Email: koczy@sze.hu
https://orcid.org/0000-0003-1316-4832

Szilvia Nagy
Department of Telecommunications
Széchenyi István University
Győr, Hungary
Email: nagysz@sze.hu
https://orcid.org/0000-0001-9556-5095

***Abstract*—In the case of computer aided diagnosis it is advantageous to apply such computational intelligence methods, that can be related to direct measured data by means easily understandable to medical experts. Fuzzy reasoning, if the rulebase is generated from plausible statistical parameters of the image to be analysed, is easy to understand thus can be easily accepted by the society.**

In the case of colorectal polyps, which might develop into colorectal cancer, thus the population-wide screening would be advisable, more methods are available, but none of them is accepted as standard and effective method. A method based on simple statistical parameters and entropies of image segments is presented, and the effect of determining the rulebase parameters on the efficiency of finding the polyp segment is studied for stabilized Koczy-Hirota rule interpolation.

***Index Terms*—Colorectal polyp, entropy, fuzzy rule interpolation, wavelet analysis**

I. Introduction

In medical practice the role of computer aided diagnosis (CAD) increases continuously. Although there are still a lot of medical experts as well as patients who have reservations about artificial intelligence, intelligent image processing and classifying methods gain application fields and appliers. It is usually complicated to understand what a medical expert wants from a computation based diagnosing aid, and also it is not simple to make them understand what an algorithm does. Although convolutional neural networks and deep learning methods are usually effective in image processing, in the case of medical diagnosis, there are several reasons why other methods for classification, such as a fuzzy sets based inference, are more advisable. One of the main reasons is that there are a lot of manifestations of the same kind of illness, and more types of lesions can look very similar on medical images. Usually the number of the samples for training and testing is limited, too. The reason for this can be the rareness of some diseases, the expensiveness of the medical experts to prepare the raw images and at least supervise the preparation of the samples from these raw images, the fact that the medical instrument providers usually make it complicated to extract good quality, processable images from their devices and also the legal, societal and ethical aspects of handling personal data, of proper anonymization. There are various picture databases for testing diagnosing methods, however, they are often either hard to access, or of rather low quality. The number of accessible databases and diagnosing challenges increases and most of the challenges concentrate on automatic segmentation of the images to detect as precise contour of the objects – usually one single kind of tumour –, or to detect, whether a pattern appears on the picture or not.

Colorectal polyps are such lesions that might develop into cancer very slowly, and usually they can be detected and classified according to dangerousness years before the malignity to appear. This means that if the population would be screened on annual or bi-annual basis, most of the colorectal cancer cases could be prevented by removing the polyps prone to develop to malign lesions. However, screening the population from about 50 years of age is hard to achieve for multiple reasons. One of the main reasons is that the most effective diagnosing device is the colonoscope – and endoscope used in the last part of the bowel –, which requires colonoscopes, personnel who is able to handle the endoscope, and cooperation of the patient not only during the examination, but also beforehand in cleaning the colorectal tract. A visual aid for detecting various polyp

978-1-7281-6932-3/20/$31.00 ©2020 IEEE

types would be welcome in order to decrease the number of missed polyps.

The polyps can be classified according to their shapes and locations related to the bowel wall layers as mucosa, muscular mucosa and submucosa. The classification was developed in Japan in the 1960s, and lately revised in Vienna and Paris [1], [2]. Based on molecular and microscopic properties of a large number of polyps, the morphological classification has 3 main classes, protruded, flat-elevated and flat, with multiple sub-classes [3], which means that there are a lot of types of shapes that should be detected by a CAD for colonoscopes. In the case of protruding polyps, also the pit pattern can be used for determining the malignity of the lesion, a classification scheme was developed by Kudo and his coworkers [4], thus the possibility for further analysis of polyps is also open for medical image processing [5].

In grand endoscopy vision challenges a call about colonoscopy was launched [6], with 8 participants and methods ranging from end-to-end learning convolutional neural networks to handcrafted algorithm to find roundish objects based on the lighting patterns of a hemisphere. The results are still not acceptable as live video image processing CAD for helping the screening of the population, however, it seems that the handcrafted and hybrid methods can outperform end-to-end learning methods, this is the reason we started to tune our fuzzy classification method [7], [8] together with the previous gastroenterological projects and cooperations of our working group [5], [9], [10] to classify colonoscopy images [11], [12], [13].

Two consecutive colonoscopy challenge used four databases of protruding types of polyps, however, one of the databases was video, and we remained at the still picture databases CVC-Colo, [14], Etis-Larib, [15], and CVC-Clinic [16], [6]. The number of the pictures were 380, 195 and 612, the size 574×500, 1225×966, 384×288 pixels, the resolution 72, 72 and 96 dpi, and the colour depth of the RGB color pictures was 24 bit per pixel, respectively. All the images were provided with a black-and-white mask of the polyp positions.

In the first tries we studied only the first database with less success, then stated to use all three databases, separating them to image groups of the same examinations, and preparing rulebases for all image groups separately [11], [12]. The method was to cut the image into tiles, and determine, whether the tile contains polyp by fuzzy classification based on statistical parameters of the image and its wavelet transform [17], in order to prepare a basic, rough contour for an active contour method [18], [19] which can refine the results of the detection.

In the previous attempts the method for generating fuzzy rules of the two outputs “contains polyp”, “does not contain polyp” we used a very simple statistical approach; for the training set we used the mean of the measured data as the $\alpha = 1$ cut point of the triangular rule, while the support was generated from the minimum and maximum measured value of the training set’s part corresponding to the respective consequent. As the support of the resulting rules of the tiles with polyp were very often included into the supports of the non-polyp rules, and the $\alpha = 1$ points were often also near, we provide an analysis in the following article about the histogram of the antecedents, and how a rulebase reproducing the histogram better than the previous, very simple method influences the output of the results. The results for the 81 image groups with the 81 different rulebases (all rulebases tested for all the rules, the colors meaning the rulebase) are presented in Fig. 1. Also the results of a joint, single rulebase based on the statistical data of the training set consisting of the training sets of all the image groups can be seen. It is visible that in most of the cases the fuzzy inferences with rulebases of separate image groups outperform that of the joint rulebase, not only for the group the rules were generated from, but also for most of the other groups. This implies that there are some groups that need different method for classification, and distort the statistics of the measured data, thus it seems to be interesting to study the distribution of the antecedents, but it is a task for a separate research. However, in this paper, as it is easier to handle the uniform rulebase, and in the long-term we are planning to apply a single, common rulebase, in the present article we study only the performance of classification the joint rulebase. The reason for trying to develop a uniform classification scheme is in the application: live video image classification needs very rapid and simple algorithms.

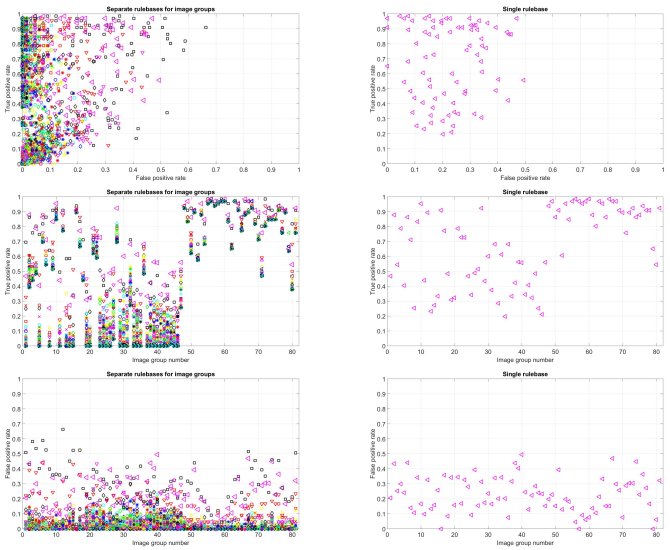

Fig. 1. True positive rates and false positive rates of the stabilized Kóczy-Hirota fuzzy rule interpolation based colonoscopy image classification. First column: the results for all the 81 image groups, of which the first 18 belongs to CVC-Colon, the next 36 belongs to CVC-Clinic, and the last 36 belongs ti ETIS-Larib. The different colors mean rulebases based on training sets from different image groups. Second column: the results for a joint, common rulebase. The magenta larger triangles of the second column are also visible in the graphs of the first column, for comparison.

In the following consideration, after a short summary of the applied rule interpolation method and the derivation of the antecedents from the raw image tiles in Section II, the histograms and the statistical parameters of the antecedents are studied in Section III. The classification results are compared in Section IV, and the conclusions are drawn in he last section.

II. Methods

Zadeh's fuzzy sets [20], [21] are often used not only in control theory and applications, but in other branches of inference, such as classification based on measured data.

A. Fuzzy rule interpolation

However Mamdani-like fuzzy inference systems [24] are proven to be successful in decision making, their possibilities are limited. In case of sparse rule bases, when the observation is between the supports of two neighbouring antecedent sets of the same dimension the weight of all rules are 0, so these applications are not able to provide any result different from zero. Its reason is the monotonity of t-norms

$$a \leq b \rightarrow t(a,b) \leq a \mid a,b \in [0,1],$$

where a and b are fuzzy membership values.

As the fuzzy rule base discussed in this paper is sparse, Mamdani-like inference systems are not suitable. For our problem the stabilized Kóczy–Hirota inference method (SKH) [25] was used. Considering the nearest antecedent sets, SKH creates temporary rules for the domains not covered by any antecedent set for each observations. These new rules can be used only for the cases they were created for. The method calculates the infima and suprema of the characteristic α-cuts of the new fuzzy conclusion B^* according to the Euclidean distances between the observation and the bounds of the characteristic α-cuts of the original antecedent sets and conclusion. The method itself is given by the following formulas

$$\inf\{B^*_\alpha\} = \frac{\sum_{i=1}^{2n} \left(\frac{1}{d_{\alpha L}(A^*, A_i)} \right)^k \inf\{B_{i\alpha}\}}{\sum_{i=1}^{2n} \left(\frac{1}{d_{\alpha L}(A^*, A_i)} \right)^k}$$

and (1)

$$\sup\{B^*_\alpha\} = \frac{\sum_{i=1}^{2n} \left(\frac{1}{d_{\alpha U}(A^*, A_i)} \right)^k \sup\{B_{i\alpha}\}}{\sum_{i=1}^{2n} \left(\frac{1}{d_{\alpha U}(A^*, A_i)} \right)^k},$$

where i stands for the number of the rules, k denotes the number of the dimensions, A^* the observation, A_i the antecedent sets in rule i, $d_{\alpha L}(A^*, A_i)$ and $d_{\alpha U}(A^*, A_i)$ the lower and upper bounds of the distance between the α-cuts of observation and the antecedents, and B^* stands for the corresponding fuzzy conclusion [26].

B. Antecedents

As the algorithm is to be used during live video investigation, it is necessary to have such antecedents that are easy to compute. Also, as the medical expert and some of the patients like to understand what a program in their device does, it is advisable to have such input parameters that are easy to understand. As the polyps are protruding into the bowel, even if their native color is the same as the bowel wall, their color representation is different due to lighting. The polyps have a lighter side toward the little light source built into the colonoscope, and a shadow at the opposite side. This suggests to use both the average pixel intensity, and their differences as input variables in the classification scheme.

Also the polyps have sharp contours, which can be seen on edge filtered images [27], and in gradient filtered images. We tried both the edge to pixel number ratio of the Canny filtered version of the image, and the gradient filtered image's mean and standard deviation.

We also calculated the structural entropy and spatial filling factor of the normalized pixel intensities, as these quantities are proven to give information about the shape of the distribution [29], [30], and it is effective in characterizing surfaces [31]– [33]. It is also shown, that structural entropy is different along a polyp-like object than in the case of the background patterns probable in bowels [34].

The input variables are used in the order shown in Table I.

TABLE I

The numbering of the antecedent parameters. R, G, and B means the color channel, STD the standard deviation, S_{str} is the structural entropy, $\ln q$ is the logarithm of the spatial filling factor from [29]. In the case of the wavelet transforms, LL stands for the low-pass–low-pass filter branch output, i.e., the rough details, HH for the output of the high-pass–high-pass branch, i.e., the fine details, while the LH and HL combinations denote the mixed outputs, i.e., if one of the directions is filtered with low-pass, the other with high-pass filter.

Number	Antecedent
1–2	mean and STD, R
3–4	mean and STD, G
5–6	mean and STD, B
7	edge density, R
8	edge density, G
9	edge density, B
10–11	S_{str}, $\ln q$, R
12–13	S_{str}, $\ln q$, G
14–15	S_{str}, $\ln q$, B
16–30	as 1–15, wavelet transform LL
31–45	as 1–15, wavelet transform LH
46–60	as 1–15, wavelet transform HL
61–75	as 1–15, wavelet transform HH
76–77	gradient magnitude's mean and STD, R
78–79	gradient magnitude's mean and STD, G
80–81	gradient magnitude's mean and STD, B
82–87	as 76–81, gradient direction
88–93	as 76–81, gradient x component
94–99	as 76–81, gradient y component

III. Histograms

As a first step for finding the reason why the separate rulebases of various image groups outperform the fuzzy classification with joint rulebase the histograms of the measured antecedents were plotted for the complete training set. Lot of the histograms seem very different from the shape of the applied fuzzy rules as it can be seen in Figure 2.

Figure 2 shows examples of the typical distributions. The mean value of the original tile has two wide peaks apart

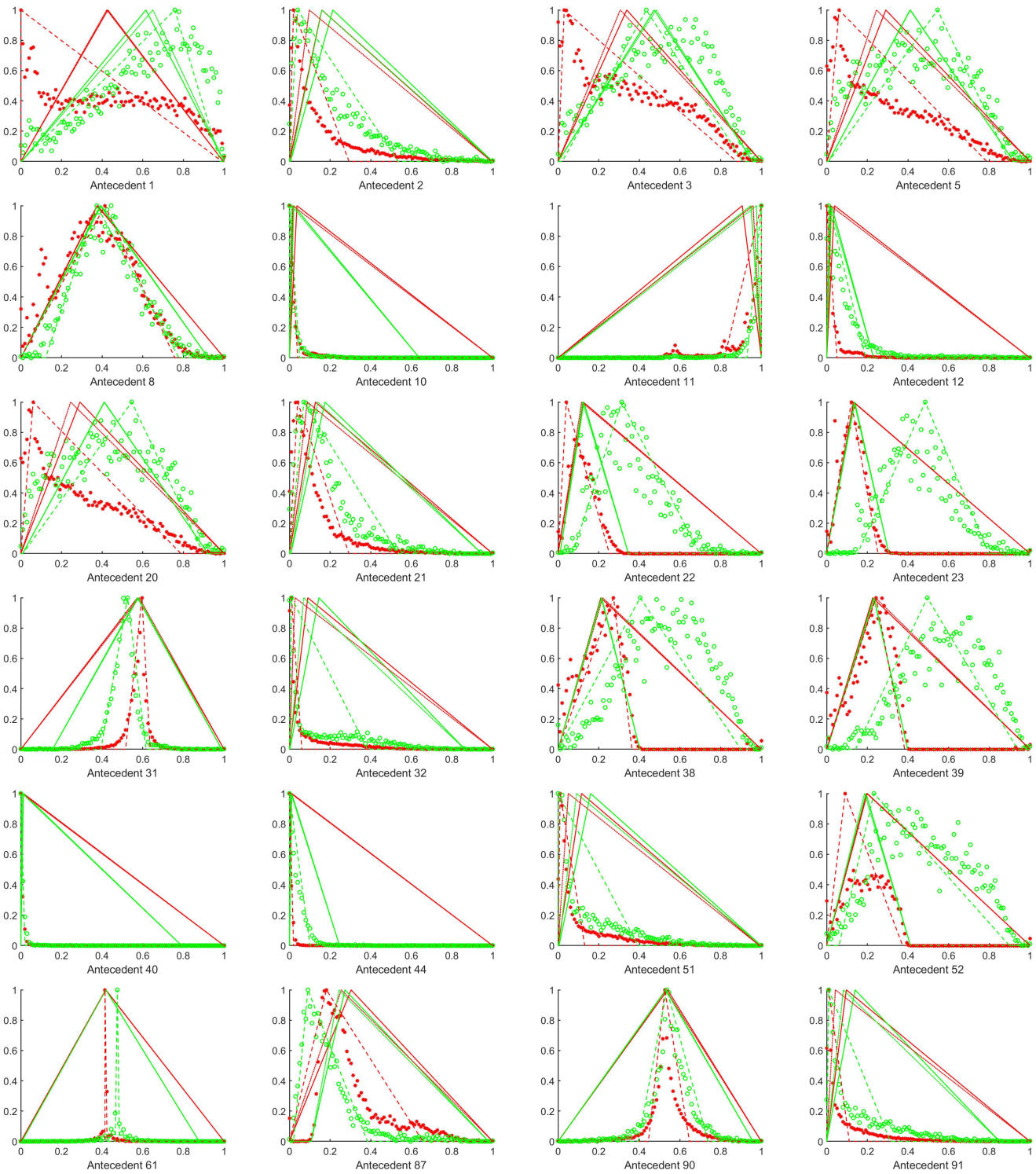

Fig. 2. Examples of histograms of the measured data in the training sets. Red color lines mean the consequent "with polyp", green color lines mean the consequent "no polyp" cases. Continuous line denotes the original rules with the mean value being the $\alpha = 1$ peak of the triangular rule, dotted line the median centered ones, and dashed line the histogram-based rules with the center being the peak of the histogram and the support set to the location where the histogram first meets the threshold level 10%. All the measured data are normalized so that the training set would be located into the closed interval $[0, 1]$, while the histogram peaks were scaled to be 1, for better visibility.

from each other for the two consequents (see No. 1, 3 and 5), while the standard deviations have almost the same peak location (see No. 2), with one of the peaks being visibly broader. The edge densities of the original form two almost overlapping wide heaps (see No. 8), while the structural entropy and the filling factor have only slightly different thin peaks at the sides of the interval, sometimes with more smaller peaks (see No. 10, 11 and 12). (This again suggests to build a hierarchical classification scheme where these entropy-based quantities play role only in some cases, even though a hierarchical classification scheme would make the calculations more complicated and time demanding.) The wavelet analysis changes the histograms of the mean values to thinner and more distinguishable peaks (see No. 20, 31 and 61), the standard deviations to slightly more fluctuating (see No. 21, 32 and 51) and the edge densities to more distinguishable (see No. 22, 23, 38, and 52). The structural entropy and the filling factor becomes even thinner (see No. 40 and 44). The gradients' mean values are usually differ only slightly in either with or peak location (see No. 90), while their standard deviations have peaks at the lower values which can be located at almost the same, or slightly different positions (see No. 87 and 91).

As the shape of the probability distributions in the training sets differ from the applied fuzzy rules very much, the goal of this research became to determine whether selecting fuzzy membership functions fitting more to the measured data improves the classification properties. Two approaches were used. First, instead of having the $\alpha = 1$ point to the mean of the measured values, it was moved to the median, which improves the fitting only slightly, as it can be seen with the dotted lines in Figure 2. This approach will be referred to as "median-centered" one in the followings. Second, in order to achieve better fitting the $\alpha = 1$ peak of the triangular membership function was set to the maximum of the histogram, while the infimum and supremum of the support was set to those points, where the histogram values first cross a given percentage of its peak value, starting from both sides of the interval $[0, 1]$. In some cases, this also resulted in bad fitting (see antecedent No. 52 in Figure 2), but mostly this fits the histograms rather well. Later this method will be called "histogram fitted" rule generation. This is the method, which produces very sparse rules, especially if the threshold for the support is set to higher levels, like the 10 % shown in Figure 2.

IV. Results compared to the original method

The performance of the method was studied by two directions: 1) how the selection of the threshold for the histogram fitting, 2) how the selection of the antecedents influences the classification results. The true positive rate (TPR), the false positive rate (FPR), the true negative rate (TNR) and the false negative rate (FNR) together classify the performance rather well, so these are the quantities given in Table II. Three representative threshold levels and 4 representative number of antecedents were selected. For selecting antecedents they were sorted according to the sum of difference magnitudes of the 3 characteristic points of the triangular membership functions, and the 66, 50 and 33 largest of these were used in the classification, respectively.

It can be seen, that the positioning of the $\alpha = 1$ point of the triangular membership function to the median of the measured data improves the performance slightly for the "yes polyp" case but makes more tiles without polyp segment be detected as polyp containing one. Also using the histogram fitted rulebases gives a bit better performance, but only, if the support is not selected to be too small.

Decreasing the number of antecedents, and thus getting rid of those input parameters that have more similar probability distributions for the two consequents can also improve the results: the 3 antecedent setup with the lowest threshold provides the best performance. The case was not studied for individual image groups yet, and also the hierarchical classification system needs to be developed in the future, as we hope, that the relation between the behaviors of the individual image-group based rulebases related to the joint rulebase is similar to that of Figure 1.

TABLE II
CLASSIFICATION PERFORMANCE FOR THE DIFFERENT METHODS WITH DIFFERENT NUMBER OF ANTECEDENTS SELECTED FOR THE CLASSIFICATION.

Method	TPR[a]	TNR[b]	FPR[c]	FNR[d]
	Number of antecedents: 99			
Original	0.82	0.46	0.54	0.18
Median centered	0.94	0.27	0.72	0.06
Histogram fitted 1%	0.79	0.49	0.51	0.21
Histogram fitted 5%	0.92	0.28	0.71	0.08
Histogram fitted 10%	0.88	0.37	0.63	0.12
	Number of antecedents: 66			
Original	0.78	0.49	0.51	0.21
Median centered	0.94	0.24	0.76	0.06
Histogram fitted 1%	0.79	0.49	0.51	0.21
Histogram fitted 5%	0.93	0.30	0.70	0.08
Histogram fitted 10%	0.87	0.37	0.63	0.12
	Number of antecedents: 50			
Original	0.72	0.56	0.43	0.28
Median centered	0.77	0.53	0.47	0.23
Histogram fitted 1%	0.82	0.45	0.55	0.18
Histogram fitted 5%	0.77	0.52	0.48	0.23
Histogram fitted 10%	0.87	0.38	0.62	0.13
	Number of antecedents: 33			
Original	0.32	0.84	0.16	0.68
Median centered	0.32	0.84	0.16	0.68
Histogram fitted 1%	0.78	0.51	0.49	0.22
Histogram fitted 5%	0.73	0.56	0.44	0.27
Histogram fitted 10%	0.87	0.39	0.61	0.13

[a]true positive rate,[b]true negative rate,
[c]false positive rate,[d]false negative rate.

V. Summary and conclusions

Stabilized Kóczy-Hirota rule interpolation based method for classifying colonoscopy image segments based on their polyp content was studied. The antecedents consisted of easily calculable parameters of the image tile and its first wavelet transform, like mean and standard deviation of the pixel intensities, edge density and the Pipek–Varga structural entropy and the gradient filtered image's mean and standard deviation values.

After studying the histograms, three rule generation methods were tested, all three provided triangular rules. The first and second method had supports for the membership functions that are located between the minima and he maxima of the measured data corresponding to the given antecedents, the third between those points where the histogram values first crossed a given threshold from both sides of the interval. The $\alpha = 1$ peak of the triangular membership functions were located to the mean, median of the measured data, and to the peaks of the histograms, respectively.

True positive and false positive rates were measured, for all the 99 antecedents and also for lower number of antecedents, where those antecedents were prioritized that had more different membership functions for the two consequents. The conclusion can be that fitting the shape of the fuzzy membership function does not improve the classification method so much as it seemed to be promising.

VI. Acknowledgements

The project was financially supported by National Research, Development and Innovation Office (NKFIH) K108405, K124055. Financial support of the Higher Education and Industry Cooperation Center at the Széchenyi University GINOP-2.3.4-15-2016-00003 is gratefully acknowledged.

References

[1] R. J. Schlemper, R. H. Riddell, Y. Kato, et al., *The Vienna classification of gastrointestinal epithelial neoplasia*, Gut, Vol. 47, pp. 251-5, 2000.

[2] H. Inoue, H. Kashida, S. Kudo, M. Sasako, T. Shimoda, H. Watanabe, S. Yoshida, M. Guelrud, C. Lightdale, K. Wanget al., *The parisendoscopic classification of superficial neoplastic lesions: esophagus,stomach, and colon: November 30 to december 1, 2002*, Gastrointest. Endosc, Vol. 58, pp. S343, 2003.

[3] R. J. Schlemper, I. Hirata, M. F. Dixon, *The Macroscopic Classification of Early Neoplasia of the Digestive Tract*, Endoscopy, Vol. 34, pp. 163168, 2002.

[4] S. Kudo, S. Hirota, T. Nakajima, et al., *Colorectal tumours and pit pattern*. J Clin Pathol, vol. 47, pp.880-885, 1994.

[5] I. Rácz, A. Horváth, M. Szalai, Sz. Spindler, Gy. Kiss, H. Regőczi, Z. Horváth, *Digital Image Processing Software for Predicting the Histology of Small Colorectal Polyps by Using Narrow-Band Imaging Magnifying Colonoscopy*, Gastrointestinal Endoscopy, Vol. 81, p. 259, 2015

[6] Jorge Bernal, et al., *Comparative Validation of Polyp Detection Methods in Video Colonoscopy: Results from the MICCAI 2015 Endoscopic Vision Challenge*. IEEE Transactions on Medical Imaging, Vol. 36, pp. 1231–1249, 2017.

[7] Sz. Nagy, F. Lilik, L.T. Kóczy, *Applicability of various wavelet families in fuzzy classification of access networks' telecommunication lines*, FuzzIEEE 2017 Naples, Italy, 9-12 July, 2017.

[8] F. Lilik, J. Botzheim, *Fuzzy based Prequalification Methods for EoSHDSL Technology*, Acta Technica Jaurinensis, Vol. 4 No. 1, pp. 135-144, 2011.

[9] I. Rácz, M. Jánoki, and H. Saleh, *Colon Cancer Detection by Rendezvous Colonoscopy: Successful Removal of Stuck Colon Capsule by Conventional Colonoscopy*, Case Rep. Gastroenterol., Volume 4, Karger, 2010, pp. 1924.

[10] V.M. Georgieva, Sz. Nagy, E. Kamenova, A. Horváth, *An Approach for Pit Pattern Recognition in Colonoscopy Images*, Egyptian Computer Science Journal Vol. 39, 201572-82, 2015.

[11] Sz. Nagy, F. Lilik, L. T. Kóczy, *Entropy based fuzzy classification and detection aid for colorectal polyps*, IEEE Africon 2017, Cape Town, South Africa, 15-17 September 2017.

[12] Sz. Nagy, F. Lilik, L. T. Kóczy, *On fuzzy classification with interpolation of the sparse rule bases*, ESCIM 2017, Faro, Portugal, 6-8 October 2017.

[13] Sz. Nagy, F. Lilik, L.T. Kóczy, *The effect of image feature qualifiers on fuzzy colorectal polyp detection schemes using KH interpolation – towards hierarchical fuzzy classification of coloscopic still images*, WCCI-FuzzIEEE 2018, Rio de Janeiro, Brasil, 8-13 July, 2018.

[14] J. Bernal, F. J. Sanchez, F. Vilariño. *Towards Automatic Polyp Detection with a Polyp Appearance Model*, Pattern Recognition, Vol. 45, pp. 31663182, 2012.

[15] J.S. Silva, A. Histace, O. Romain, X. Dray, B. Granado, *Towards embedded detection of polyps in WCE images for early diagnosis of colorectal cancer*, Int J Comput Assisted Radiology and Surgery, Vol. 9, pp. 283-293, 2014.

[16] J. Bernal, F. J. Sanchez, G. Fernndez-Esparrach, D. Gil, C. Rodrígez, F. Vilariño, *WM-DOVA maps for accurate polyp highlighting in colonoscopy: Validation vs. saliency maps from physicians*, Computerized Medical Imaging and Graphics, Vol. 43, pp. 99-111, 2015.

[17] I. Daubechies, *Ten Lectures on Wavelets*, CBMS-NSF regional conference series in applied mathematics 61, SIAM, Philadelphia, 1992.

[18] M. Kass, A. Witkin, D. Terzopoulos, *Snakes: Active contour models*, Int J Comput Vision Vol. 1, pp. 321-331, 1988. https://doi.org/10.1007/BF00133570

[19] V.M. Georgieva, S.G. Vassilev, *Kidney Segmantation in Ultrasound Images via Active Contours*, 11th International Conference on Communications, Electromagnetics and Medical Applications, Athens, Greece, October 2016.

[20] L. A. Zadeh: *Fuzzy sets, Information and Control*, vol. 8, pp. 338-353, 1965.

[21] L. A. Zadeh: *Fuzzy algorithms*, Information and Control, vol. 12, pp. 94-102, 1968.

[22] L. T. Kóczy, K. Hirota, Approximate reasoning by linear rule interpolation and general approximation, International Journal of Approximate Reasoning, vol. 9, 1993, pp. 197–225, doi: 10.1016/0888-613X(93)90010-B

[23] L. T. Kóczy, K. Hirota, Interpolative reasoning with insufficient evidence in sparse fuzzy rule bases, Information Sciences, vol. 71, 1993, pp. 169–201, doi: 10.1016/0020-0255(93)90070-3

[24] E. H. Mamdani, S. Assilian: An experiment in linguistic synthesis with a fuzzy logic controller, International Journal of Man-Machine Studies, vol. 7, 1975, pp. 1–13, doi: 10.1016/S0020-7373(75)80002-2

[25] D. Tikk, I. Joó, L. T. Kóczy, P. Várlaki, B. Moser and T. D. Gedeon, Stability of interpolative fuzzy KH-controllers, Fuzzy Sets and Systems, vol. 125, 2002, pp. 105–119, doi: 10.1016/S0165-0114(00)00104-4

[26] K. Balázs, L. T. Kóczy, Hierarchival-Interpolative Fuzzy System Construction by Genetic and Bacterial Memetic Programming Approaches, International Journal of Uncertainty, Fuzziness and Knowledge-Based Systems, vol. 20, 2012, pp. 105–131, doi: 10.1142/S021848851240017X

[27] R. Maini, H. Aggarwal, *Study and Comparison of Various Image Edge Detection Techniques*, Int J Image Processing (IJIP), Vol. 3 p. 1, 2009.

[28] J. Canny, *A Computational Approach To Edge Detection*, IEEE Trans. Pattern Analysis and Machine Intelligence, Vol. 8, pp. 679698, 1986.

[29] J. Pipek and I. Varga, *Universal classification scheme for the spatial localization properties of one-particle states in finite d-dimensional systems*, Phys. Rev. A, Volume 46, APS, Ridge NY-Washington DC, 1992, pp. 3148–3164.

[30] I. Varga and J. Pipek, *Rnyi entropies characterizing the shape and the extension of the phase space representation of quantum wave functions in disordered systems*, Phys. Rev. E, Volume 68, APS, Ridge NY-Washington DC, 2003, 026202.

[31] L. M. Molnár, Sz. Nagy, and I. Mojzes, *Structural entropy in detecting background patterns of AFM images*, Vacuum, Volume 84, Elsevier, Amsterdam, 2010, pp. 179-183.

[32] A. Bonyár, L. M. Molnár, G. Harsányi, *Localization factor: a new parameter for the quantitative characterization of surface structure with atomic force microscopy (AFM)*, MICRON, Volume 43, Elsevier, Amsterdam, 2012, pp. 305-310.

[33] A. Bonyár, *AFM characterization of the shape of surface structures with localization factor*, Micron, Vol. 87, pp. 1-9, 2016.

[34] Sz. Nagy, B. Sziová, J. Pipek, *On Structural Entropy and Spatial Filling Factor Analysis of Colonoscopy Pictures*, Entropy, Vol. 21, 256, 32 pages, 2019.